

# Installation and test of the fiber link to 1.5m echelle

A. Tokovinin

Version 1. April 25, 2008  
file: prj/bme/doc/installation.tex

The installation and test was performed on April 16-18, 2008, during two technical nights. Telops staff (O. Saá, J. Briones, J. Rojas, D. Rojas, E. Cosgrove, A. Gomez) was involved, as well as the SMARTS observers J. Velasquez and M. Hernandez.

## 1 M1 mirror in the GAM

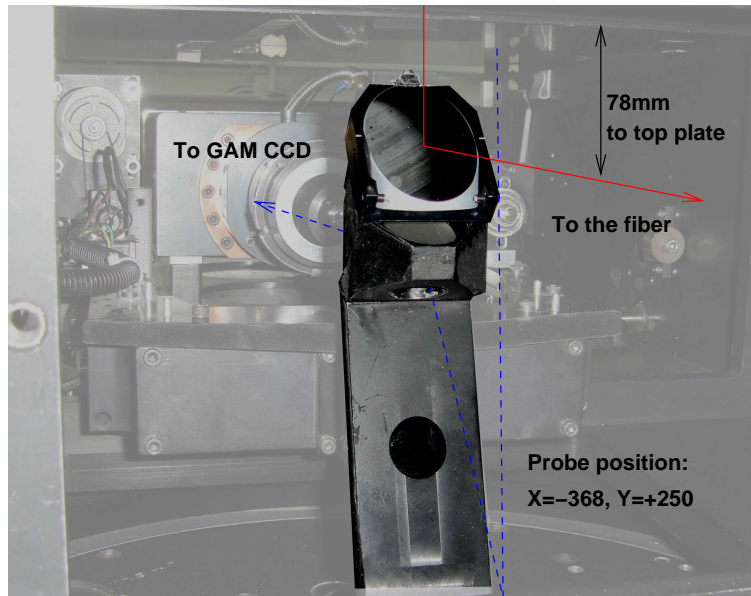


Figure 1: M1 mirror attached to the GAM probe.

The elliptical mirror M1 is attached to the top of the GAM probe arm to intercept the beam and to direct it to the Front-End Module (FEM). The mirror “sits” in its cell on two machined lower pads and one adjustment screw. It is fixed laterally by two pins (M3 set screws) and pressed against attachment points by the flexible leaf with plastic pad at the top (Fig. 1).

To install M1, the GAM was detached from the telescope and its probe was un-screwed (there are 6 screws, the camera must be moved back to access the two top screws). Two M3 threads were

machined in the back side of the probe. The M1 cell is firmly pressed by two M3 screws against the probe, without any play. The adjustment in angles is achieved by the two M2 set screws on the back (in horizontal direction) and the M3 adjustment screw (up-down). The M1 does not perturb the normal operation of the GAM probe. However, to direct the light to the fiber, the probe must be set in a fixed position at  $X = -368$ ,  $Y = +250$ . Thus, it is not possible to search for the guide stars with GAM. Increasing  $X$  moves the probe to the right (when looking through the hatch door), increasing  $Y$  approaches it to the door. By moving in  $Y$  200 steps back (to +50), we can acquire the same object in the GAM camera.

The optical axis of the fiber light path is at 78 mm below the lower surface of the GAM top plate. The M1 was aligned initially with a laser beam going along this axis, reflecting off M1 and then back from a small flat mirror parallel to the top plate. Later, during the day, the alignment was refined by looking through the FEM (with the telescope pointing to the sky) and avoiding vignetting. It is possible to do so only with the GAM counter-weight removed. The flexible leaf must be released during this alignment, then tightened again. This leaf is actually tricky, as it can push M1 off its alignment screw when tightened (to be corrected later).

The Y-position of the arm moves the star in the field and changes the focus. It was refined by first centering the star on the slit of the RC spectrograph. Then the probe was moved in and the star was centered in the FEM field at  $Y=+250$ . The focus of FEM and RC spectrograph is nearly coincident (focus reading around 58).

Defocused images of stars in the TV guider did show substantial vignetting, even close to the center. Further tests are needed to ensure the absence of vignetting in the FEM optical path.

## 2 Attaching the Front-End Module to the GAM

The hatch door of the GAM was modified for FEM attachment: a 42-mm hole at 57 mm from its upper edge (or 78 mm below the top plate) was machined, four M4 threads were made, and the handling knob added. Figure 2 shows the FEM attached to the hatch door and placed on the GAM (the counter-weight is removed). As the space is restricted and the access to FEM is difficult, it was planned to remove it together with the door for any operations. This is possible only without the counter-weight. To increase the space, the lower plate of the counter-weight was reduced by 100 mm and the knob of the GAM rotation clamp (protruding down in the upper-right of Fig. 2) was reduced as well. Even though, it turned difficult or impossible to remove FEM with the hatch door. So, the holes in the FEM were modified to permit its easy removal from the hatch door. In the future, an even simpler attachment with a clamp may be designed.

## 3 Comparison lamps

The comparison lamps and their power supplies will be mounted at the telescope, in a common housing. This has not been done yet, so the “light box” and its supplies was temporarily located near the telescope for taking comparison spectra.

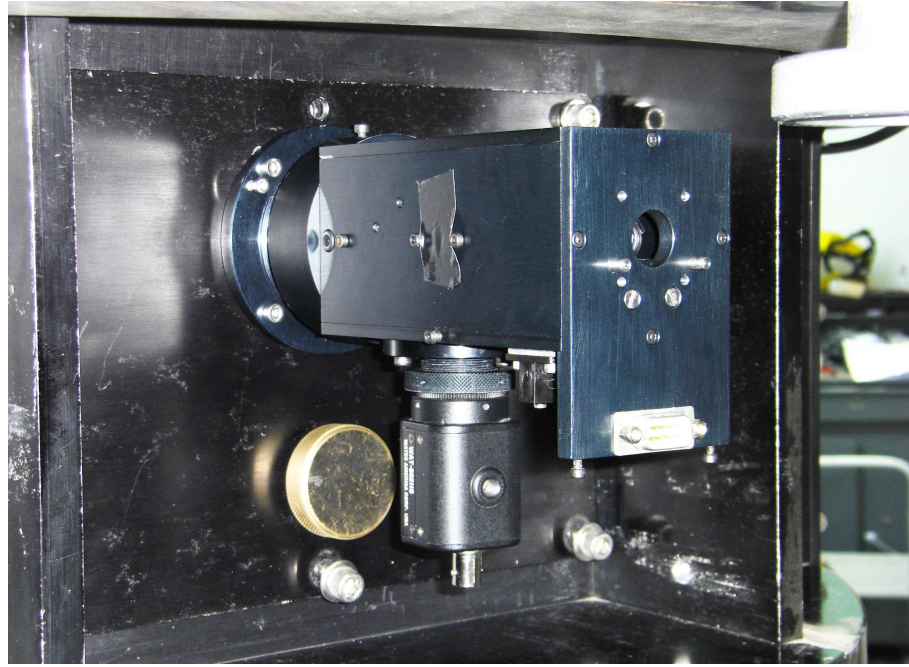


Figure 2: FEM attached to the GAM door.

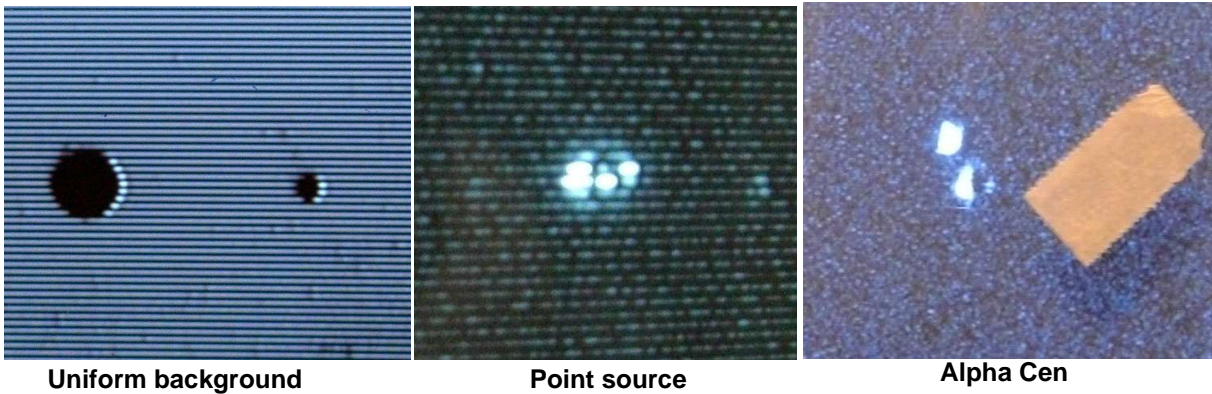


Figure 3: Photographs of the TV guiding screen in three different situations.

## 4 Guiding

The video signal from the guiding TV camera is brought to the control room by a coaxial cable (though the patch line RF1) and displayed on the monitor. Figure 3 shows that the image of the holes in M2 is very sharp (good guider optics). The diameter of the small hole (where the star should be located) is about 4 TV lines. The large hole (for sky fiber) is not used. When a point source (simulated with laser) is centered in the small hole, we see only the halo and, if the source is faint enough, the hot pixels. The hot pixels will help to locate the hole on the screen, as it is not visible on the dark sky.

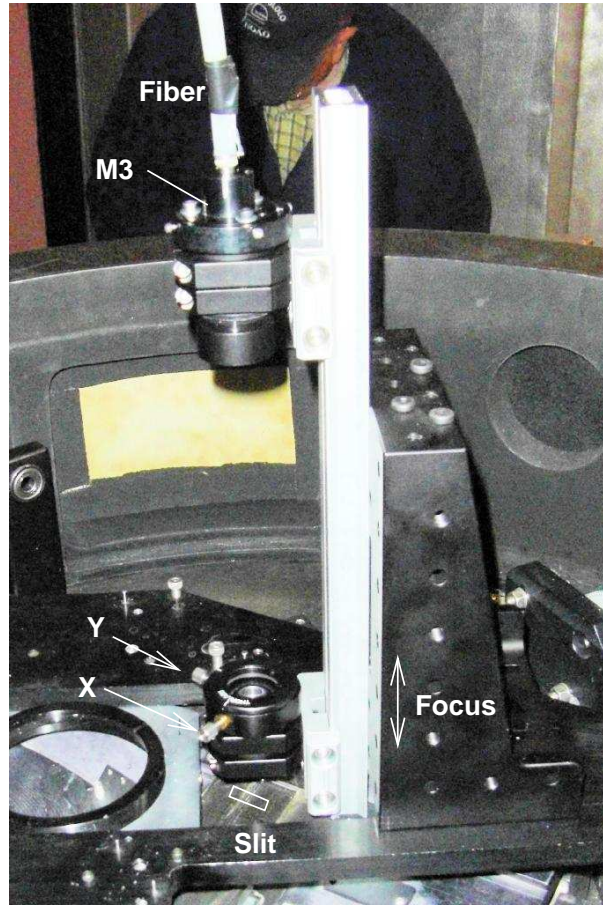


Figure 4: Back-End Module at the spectrograph.

During the first tests on April 16, the problem of saturation became apparent. The automatic exposure control does not adjust the exposure on point sources, so bright stars are strongly saturated. In desperation, I set the TV exposure to fixed values. The 2 ms exposure works for stars of  $V=8$  magnitude, the shortest ( $10 \mu\text{s}$ ) is acceptable for  $\alpha$  Cen. The total range of exposures (from  $10 \mu\text{s}$  to 20 ms) is about  $8^m$ . However, manual setting of exposure is not a valid option for observations.

After these tests, I installed the additional light source (LED) in the instrument. It illuminates the right side of the field and shortens the exposure. Tests with the simulated star have shown that this method works. In addition, I installed two neutral filters (optical density 2 each), to be inserted manually if needed. If these filters prove to be necessary, at least one can be motorized.

To our surprize, there were sufficiently bright stars in the GAM fields adjacent to some targets. In these cases, it is possible to use the existing GAM guiding, after centering the star in the hole. This works for  $\alpha$  Cen.

## 5 Back-end module

The Back-End Module (BEM) is mounted on the front plate of the Blanco Echelle Spectrograph by means of the AR90 angular bracket, attached to the plate with two 1/4 screws (Fig. 4). The bracket holds the rail with two carriages. The upper carriage holds the 50-mm focus lens and fiber cable. The cable must be inserted and fixed by tightening the M3 set screw. This assembly is pre-aligned to give a parallel and well-centered beam. The diameter of the collimated beam is about 10 mm.

The lower carriage holds the 75-mm focus lens which re-focuses the fiber-end image on the slit. The magnification is 1.5x, so the image diameter is  $150\ \mu\text{m}$ . The slit is  $\sim 42\ \text{mm}$  below the surface of the front plate, its orientation is indicated in Fig. 4. The X and Y knobs permit to move the image on the slit in, respectively, perpendicular and parallel directions. The image is focused by moving the whole lower carriage along the rail.

With the fiber illuminated (sky through the telescope or quartz lamp), the image is focused and centered by looking in the post-slit viewer. Initially the slit is wide, then it is set to the desired width (between  $60\ \mu\text{m}$  and  $150\ \mu\text{m}$ ), with the smallest decker.

## 6 Spectrograph setting and focus

The echelle grating is 31.6 l/mm, the cross-disperser is number-2, 226 l/mm. The angle of the echelle is 568, set to center the blaze function on the detector. Fig. 5 shows that this centering is good. The collimator focus is 99.80.

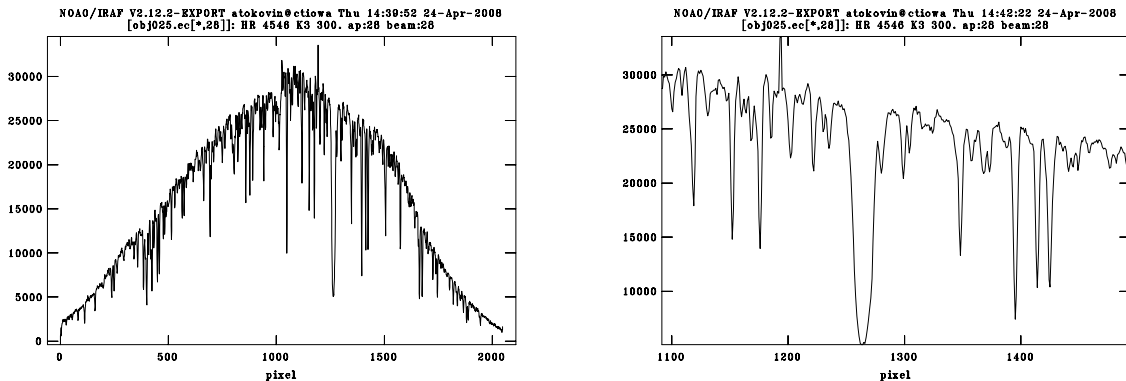


Figure 5: Plots of the extracted spectra of HR 4546 around  $H\alpha$  (left – the whole order, right – zoom on  $H\alpha$ ). The spectrum has not been flat-fielded, the difference in the response between two amplifiers (left and right halves) is apparent.

The cross-disperser is apparently blazed for long wavelengths, and should be changed to grating 3. Its angle was set to 1120 during night-time tests, then changed to 1114 to move the spectrum upwards (get shorter wavelengths, as red is “up”). As the spectrograph has not been tuned after its re-location, the results are still very preliminary. Fortunately, the focus was not too bad (the best FWHM of Th lines is around 2 pixels). The detector controller was not very stable (there are differences between the bias images).

All frames were converted to FITS (IRAF command `wfits`) and translated to `ciowa` by FTP. Overscan was subtracted and trimmed, bias was subtracted using the IRAF task `quadproc`. The echelle orders were traced and the spectra extracted. No other processing was done. The order FWHM in the cross-dispersion direction is 3.3 pixels, the distance between the orders in the blue (shortest) is 20 pixels. The dispersion around Na doublet (5900Å) is 0.067 Å/pixel, which corresponds to the 2-pixel resolution  $R = 43700$ .

On April 19, the spectrograph focus was checked with the mask covering, in turn, west or east half of the collimator. The slit width was set to 60 μm (narrower than the fiber image). This test was interrupted by unexpected detector warming and continued later after dewar refill and cooling down to 165.5 K (nominal CCD temperature). The frames `obj157` and `obj158` are obtained with 120 s exposure one after another with two mask positions.

The mask data are processed with the IDL program `focus.pro` written for this purpose. It is based on the `find` procedure from IDLPHOT package which finds all star-like features. The limits on sharpness are 0.2–0.75, on roundness from 0 to 1.5, to avoid defects as much as possible. All lines with flux greater than 10 000 ADU are discarded, leaving about 1000 identifications per frame. Then the lines are matched by finding, for each feature, the closest one in the second frame. The upper distance limit for matching is set to 5 pixels. There were 504 matched pairs. The difference of their X-coordinates (along dispersion)  $\Delta x$  is interpreted as defocus. The true defocus  $\Delta l$  is estimated as  $\Delta l \approx \Delta x p (2F/D)$ , where  $p = 24 \mu\text{m}$  is the pixel size,  $F = 590 \text{ mm}$  and  $D = 100 \text{ mm}$  are the spectrograph camera focal length and diameter. The defocus  $\Delta x(X, Y)$  is approximated by the 2-nd order surface, with the residuals mostly less than 0.5 pixels. Figure 6 shows this surface.

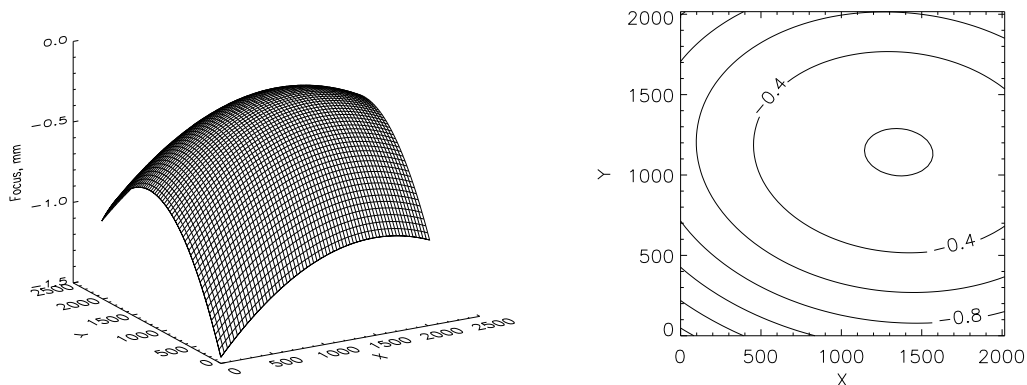


Figure 6: Second-order surface describing the defocus of the spectrograph (left – in isometric view, right – contour plot).

The curvature of the focal surface corresponds to the curvature of the Schmidt camera focal plane (curvature center at  $2F$  from the detector). So, negative defocus values tell us that the detector must be further away from the camera by  $\sim 0.5 \text{ mm}$ . Currently the CCD dewar focus reading is 1.430, The dewar distance from the camera flange is 43.0 mm. The tilt in X must be adjusted, too. The best compromise focus is yet to be established to obtain the narrowest lines over relevant parts of the echelle orders.

## 7 Total efficiency

Test spectra of three bright stars obtained on Aril 17 permit to make first estimates of the total system efficiency  $\epsilon = F_{det}/F_{incident}$ , where  $F$  are the flux spectral densities in photons/(Å s), incident (outside atmosphere) and detected. The crude estimate  $F_{incident} = S 10^{3-0.4V}$  is used, with  $V$  being the visual magnitude of the star and  $S$  the telescope surface. The flux in the extracted spectrum  $F_{ADU}$  is converted from ADU to photons using the formula  $F_{det} = F_{ADU} g/(\delta\lambda t)$ , with the gain  $g = 1.4 \text{ el/ADU}$ , pixel resolution  $\delta\lambda = 0.067 \text{ \AA}$ , and exposure time  $t = 300 \text{ s}$ .

The detected flux was measured near the center of the blaze function to the left of the Na doublet. The Table below lists the resulting system efficiency estimates.

HR	V	Sp	F_ADU	F_det	F_incident	Epsilon, %
4546	4.46	K3III	16000	1114	2.91E5	0.38
4494	4.70	B9V	8200	571	2.33E5	0.25
4775	4.31	F2V	12000	835	3.34E5	0.25

For reference, the efficiency of the echelle spectrograph on the 2.5-m DuPont telescope estimated by the same method is 7.7%. The exposure time calculator for the KPNO echelle spectrograph (identical to the Blanco echelle) leads to the numbers between 3% and 6%, depending on the cross-disperser. Clearly, the efficiency of the 1.5-m echelle system needs to be improved. Experiments to characterize each component on the light path, up to the detector gain, must be planned and executed. One obvious source of the light loss is the non-optimal cross-disperser.

## 8 To-do list

- Test vignetting in the FEM light path
- Test guiding on bright and faint stars
- Fabricate and test the control electronics box, install it with the light box on the telescope
- Align the spectrograph
- Measure the spectrograph efficiency
- Measure the detector gain and quantum efficiency